Article

Journal of Industrial Textiles

2022, Vol. 51(2S) 3219S–3237S

DOI: 10.1177/15280837211054218
journals.sagepub.com/home/jit
SAGE

Engineered properties of polyurethane laden with beetroot and cerium oxide for cardiac patch application

Saravana Kumar Jaganathan[1,2], Mohan Prasath Mani[3], Ahmad Fauzi bin Ismail[4], Ahmad Zahran Mohd Khudzari[5], Ahmad Athif Mohd Faudzi[2,6]

Abstract

The cardiac patch provides appropriate physicochemical properties and mechanical strength for the regeneration of damaged heart tissues. In this work, for the first-time, beetroot (BR) is blended with cerium oxide (CeO_2) to produce nanofibrous polyurethane (PU) composite patch using electrospinning. The objective of this work is to fabricate the composite and examine its feasibility for cardiac patch applications. Morphological analysis revealed a dramatic reduction of fiber diameter of PU/BR (233 ± 175 nm) and PU/BR/CeO_2 (331 ± 176 mm) compared to the pristine PU (994 ± 113 mm). Fourier transform infrared analysis (FTIR) analysis indicated functional peak intensities of the newly formed composite PU/BR and PU/BR/CeO_2 were not similar to PU. The addition of beetroot rendered PU/BR hydrophilic (86° ± 2), whereas PU/BR/CeO_2exhibited hydrophobic nature (99° ± 3). Atomic force microscopy (AFM) analysis depicted the reduced surface roughness of the PU/BR (312 ± 12 nm) and PU/BR/CeO_2 (390 ±

[1]Department of Engineering, Faculty of Science and Engineering, University of Hull, Hull, UK
[2]School of Electrical Engineering, Faculty of Engineering, Universiti Teknologi Malaysia, Johor Bahru, Malaysia
[3]School of Biomedical Engineering and Health Sciences, Faculty of Engineering, Universiti Teknologi Malaysia, Skudai, Malaysia
[4]Advanced Membrane Technology Research Centre (AMTEC), School of Chemical and Energy Engineering, Universiti Teknologi Malaysia, Skudai, Malaysia
[5]IJN-UTM Cardiovascular Engineering Center, School of Biomedical Engineering and Health Sciences, Faculty of Engineering, UniversitiTeknologi Malaysia, Skudai, Malaysia
[6]School of Electrical Engineering, Centre for Artificial Intelligence and Robotics, Universiti Teknologi Malaysia, Kuala Lumpur, Malaysia

Corresponding author:
Saravana K Jaganathan, Department of Engineering, Faculty of Science and Engineering, University of Hull, Hull HU6 7RX, UK.
Email: s.k.jaganathan@hull.ac.uk; jaganathaniitkgp@gmail.com

125 nm) than the pristine PU (854 ± 32 nm). The incorporation of beetroot and CeO_2 into PU enhanced the tensile strength compared with the pristine PU. The blood clotting time of PU/BR (APTT-204 ± 3 s and PT-103 ± 2 s) and PU/BR/CeO_2 (APTT-205 ± 3 s and PT-105 ± 2s) were delayed significantly than the pristine PU(APTT-176 ± 2 s and PT-94 ± 2 s) as revealed in the coagulation study. Further, hemolysis assay showed the less toxic nature of the fabricated composites than the pristine PU. Hence, it can be inferred that the advanced physicochemical and blood compatible properties of electrospun PU/BR and PU/BR/CeO_2 nanocomposite can be engineered successfully for cardiac patch applications.

Keywords
PU, CeO_2, beetroot, electrospun scaffold, cardiac applications

Introduction

Myocardial Infarction (MI) and heart failure are the foremost causes for death globally. MI occurs when blood flow to the heart is reduced causing blockage of coronary arteries leading to heart muscle damage.[1] MI is followed by several events like inflammatory responses, cardiomyocyte death, the formation of scar, infracted region expansion, and left ventricular wall thinning.[2,3] The heart fails to function along with these events and in the final stages, there will be concomitant arrhythmias and mitral regurgitation resulting in cardiac failure.[4,5] Heart transplantation is the golden standard for overcoming cardiac failure, however, the scarcity of donors' forces physicians and researchers to look for other viable alternative routes.[6] Standard treatments/therapies such as thrombolytic/fibrinolytic therapy, coronary angioplasty, and coronary artery bypass grafting were used in remodeling of the damaged heart muscle. However, these are not efficient in repairing the cardiac tissue.[7–9] The usages of a cardiac patch for regenerating damaged tissues is experimented and there is a vast potential for the advanced material to aid this problem.[10] The hourly need for the cardiac patch materials motivated material scientists to collaborate with physicians to develop and experiment with new materials. The key aspect of the search is that the new materials should bio-mimic the properties of the heart extracellular matrix and support the cardiomyocyte adhesion and proliferation for new tissue growth.[11]

To achieve this, several ways were utilized to fabricate the cardiac patch materials. One of the versatile and economic modes of fabricating such material is electrospinning.[12] A typical electrospinning apparatus set up mainly consists of three components, namely, high electric field, collector drum, and syringe pump.[13] The electrospinning technique uses high voltage to convert the polymeric solution loaded in the syringe pump into fibers which are collected at the collector drum.[14] Fibers produced through the electrospinning technique possess tremendous advantages such as large specific surface area and porous structure grossly mimicking the extracellular matrix (ECM) which makes them a widely accepted choice for tissue engineering applications.[15–17] Recently, polymeric scaffolds play a vital role in tissue engineering applications.[18] The characteristics and properties of

polyurethane are ease of processing, flexibility, biocompatibility, biodegradable, haemocompatibility, and tailorable chemical and physical forms.[19] Few works highlighted the usage of electrospun polyurethane fibers for tissue engineering applications.[20,21] Polyurethane has been blended with various molecules in order to improve its bioactivity behavior for tissue engineering applications. Few literatures reported the usage of nanoparticles incorporated PU scaffold for tissue engineering applications.[22,23] Cerium oxide is reported to be beneficial in reactive oxygen species scavenging[24] and also possesses antioxidant behavior.[25] Cerium oxide-loaded scaffolds holds potential in the biomedical field[26] and their application is limited due to toxicity.[27] Fruits and vegetables contain wide sources of minerals, nutrients, vitamins, folic acid, and dietary fiber. Some components of fruits and vegetables (phytochemicals) possesses strong antioxidants behavior. Further, the phytochemicals present in the fruits and vegetables have a complementary mechanism which include antibacterial and antiviral effects, scavenging of free radicals, promotes cell adhesion, proliferation, and differentiation and hormone metabolism regulation.[28] We hypothesize by blending with natural root vegetables like beetroot would be beneficial in overcoming this drawback of cerium induced toxicity to the tissue engineering scaffolds. Hence, this work for the first time attempts to combine cerium oxide with beetroot to develop a cardiac patch using electrospinning.

Beetroot (*Beta vulgaris* L.) is a vegetable plant belonging to the family Amaranthaceae.[29] Raw beetroot contains carbohydrates, protein, and fat. It provides 43 calories with a rich source of folate and a moderate source of manganese along with other nutrients.[30] It is used in cooking foods, food coloring, and also as a medicinal plant.[31] Beetroot is reported to be rich in nitrates which help in reducing the blood pressure thereby exerting benefits in protecting the cardiovascular system. Additionally, the consumption of beetroot juice exhibits cardioprotective properties because of the presence of betalains and antioxidant properties of its components.[32–34] Recent reports indicated the various biological properties of *Beta vulgaris* extracts such as antioxidant, anti-inflammatory, antihypertensive, hypoglycemic, and hepatoprotective activities.[29] However, its potential is still untapped in the field of regenerative medicine. Cerium is a rare earth metal having anatomic number 58. It belongs to the lanthanide series and occurs in two oxidation states, that is, +3 and +4. Since it belongs to the lanthanide series, it is used as a catalyst, ultraviolet absorber, gas sensors, and polishing agent. It is also used as electrode material in gas sensors because of their very good oxide ion conductors. The cerium particles were reported to possess antioxidant properties.[35] Further, few studies have been reported the low toxicity nature of cerium particles which do not induce any cytotoxicity or inflammation.[36–38] The application of cerium nanoparticles in biomedical applications is widely documented in areas such as redox modulation, drug delivery agent, pharmaceutical, treating bone cancer, and tissue engineering scaffolds.[39–41] This study aims to develop a cardiac patch based on polyurethane added with beetroot and cerium oxide using electrospinning technique and explore its physicochemical and blood coagulation properties for promoting PU/BR and PU/BR/CeO_2in cardiac patch applications.

Materials and methodology

Materials

Tecoflex EG-80A polyurethane ((molecular weight = 1000 g/mol)) was procured from Lubrizol and the solvent dimethylformamide (DMF) was purchased from Sigma Aldrich, UK. PU is a segmented polymer that has methylene bis(cyclohexyl) diisocyanate (hydrogenated MDI, H12MDI) as a hard segment and polytetramethylene oxide as a soft segment having a molecular weight of 1000 g/mol. It also contains 1,4 butane diols as a chain extender. Beetroot was obtained from local vendor. CeO_2 was procured from Sigma Aldrich, UK. Phosphate buffered saline (PBS) and sodium chloride (NaCl) physiological saline (0.9% w/v) were procured from Sigma-Aldrich, Kuala Lumpur, Malaysia. The blood clotting assay reagents such as rabbit brain-activated cephaloplastin, calcium chloride ($CaCl_2$) (0.025 M), and thromboplastin (Factor III) were purchased from Thermo Fisher Scientific, Selangor, Malaysia. All chemicals used in this work are of analytical grade.

Preparation of beetroot extract

Initially, the surface of the beetroot was peeled off fully and cleaned using distilled water. Using a common kitchen blender, it was grinded to obtain extracts from it. Finally, the filtered extract was stored in the refrigerator for further use.

Preparation of solution

Initially, PU was prepared at a concentration of 9 wt%. It was done by dissolving 360 mg in 4 ml of DMF and stirred for 12 h to attain a homogeneous solution. For BR homogeneous solution, 4 w/v% was used which was prepared by adding 120 µl of BRin 3 ml of DMF and stirred for 1 h. Similarly, CeO_2 homogeneous solution was prepared at 4 wt% by adding 120 mg of CeO_2 in 3 ml of DMF and stirred for 1 h. Finally, PU/BR and PU/BR/CeO_2 composite solutions were prepared by mixing BR and CeO_2 homogeneous solution into PU homogeneous solution at a ratio of 8:1 (v/v%) and 8:0.5:0.5 (v/v%) and stirred for 1 h maximum. The schematic representation of preparation of solution is indicated in Figure 1.

Electrospinning process

The electrospun technique was used to make the cardiac patch from the prepared PU,PU/BR, and PU/BR/CeO_2 composite solutions. In this study, the applied parameters were voltage of 10.5 kV, a flow rate of 0.2 ml/h, and the collector distance was set at 20 cm. The collected nanofibers in the aluminium foil were detached carefully and vacuum dried at room temperature.

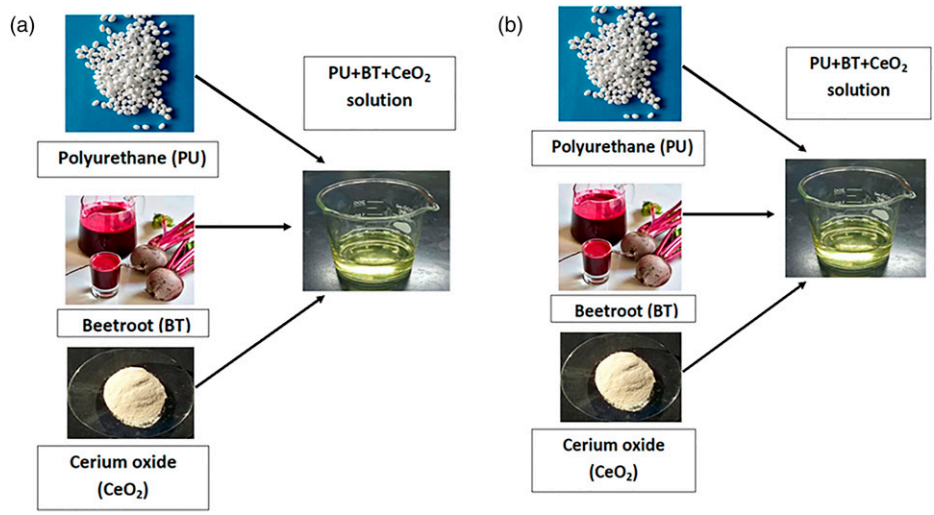

Figure 1. Schematic representation of preparation of solution.

Physicochemical characterizations

Field Emission Scanning electron microscopy (FESEM). FESEM unit (Hitachi SU8020) was utilized to investigate the morphology of the PU, PU/BR, and PU/BR/CeO_2. Before attaining photomicrographs, samples cut into small pieces were gold plated at 20 mA for 2 min. Then, the images were captured at different magnifications with an accelerated voltage of 10 kV. The fiber diameter was calculated from the captured image using Image J by choosing 30 locations randomly. The cerium oxide present in the electrospun nanofibers were determined using energy dispersive X-ray (EDX) spectrometer attached to the FESEM unit.

Fourier transform infrared (FTIR) analysis

The characteristic bands present in the PU, PU/BR, and PU/BR/CeO_2 were recorded using the Thermo Nicolet FTIR unit. ATR crystal fixed in the NICOLET IS5 spectrometer was zinc selenium (ZnSe). The sample spectra were recorded between the wavelength of 600 and 4000 cm^{-1} at 32 scans per minute with a resolution of 4 cm^{-1}.

Contact angle measurements

The surface wettability of PU, PU/BR, and PU/BR/$CeO_2$was determined using a video contact angle measurement unit. A water droplet image was deposited on the small cut mesh of the electrospun membrane and an image of the droplet laid was captured with the help of a high-resolution camera within a few seconds. The angle between the water

droplet and the surface was calculated from the captured image using computer integrated software provided by the manufacturer.

Mechanical properties test

According to ASTM standard (ASTM D882-10), the tensile strength of PU, PU/BR, and PU/BR/CeO_2 were investigated. For measuring this, samples with a rectangle size of 40 × 15mm^2 were cut and fixed in the grips of the uniaxial tester. The test was carried out at a strain rate of 10 mm/min and pulled until failure occurs. The average tensile strength was obtained from the machine generated stress–strain curve.

Thermogravimetric analysis (TGA)

TGA unit (PerkinElmer TGA 4000 unit) was used to evaluate the thermal stability of the PU, PU/BR, and PU/BR/CeO_2. All analysis was performed in a dry nitrogen atmosphere. A small piece weighing 3 mg was heated at a rate of 10°C/min with a flow rate of 50 mL/min at a temperature range of 30–1000°C.

Atomic force analysis (AFM)

AFM was performed using AFM apparatus (Nanowizard, JPK instruments) to analyze the surface properties of the PU, PU/BR, and PU/BR/CeO_2. The sample surface area was scanned in a size of 20 × 20 μm area in a normal atmosphere at room temperature. The 3D digital images with 256 × 256 pixels were captured using JPJSPM software.

Blood compatibility measurements

Activated Partial Thromboplastin Time (APTT) Assay. The cut samples of electrospun PU and its composites scaffolds were incubated with 50 μL of obtained PPP for 1 min at 37°C and then added with 50 μL of rabbit brain cephaloplastin reagent for 3 min at 37°C. Finally, the mixture was added with 50 μL of $CaCl_2$ which activates the blood clot. The time taken for the clot formation was measured using a chronometer.[42,43]

Prothrombin time (PT) assay. The cut samples of electrospun PU and its composites scaffolds were incubated with 50 μL of obtained PPP for 1 min at 37°C followed by adding 50 μL of NaCl–thromboplastin reagent (Factor III) which triggers the blood clot. The time taken for the formation of the clot is noted as PT.[42,43]

Hemolysis assay. To start this assay, the cut samples of electrospun PU and its composites scaffolds were cleaned in physiological saline (0.9% w/v) at 37°C for 30 min. After the samples were exposed to the citrated blood and diluted, saline mixture was prepared at 4:5 for 1 h at 37°C. Then, the samples were retrieved and centrifuged at 3000 r/min for 15 min. Finally, optical density (OD) was recorded for the aspirated supernatant which

measures the damage of red blood cells (RBCs). The hemolytic percentage was calculated using the following formula as reported previously.[42,43]

Statistical analysis

All experiments were performed thrice independently. To measure the statistical significance, one-way ANOVA was carried out in Graph pas prism and the calculated results are denoted as mean ± SD and for qualitative experiments, a representative of three images is shown.

Result and discussion

FESEM investigation

Figure 2 depicts the FESEM images of nanofibers made from PU and PU, PU/BR, and PU/BR/CeO_2. All three samples had nanofibers with smooth and randomly oriented fibers without any beads. ImageJ analysis depicted the average diameter of the pure PU measured was found to be 994 ± 113 nm, while PU/BR and PU/BR/CeO_2 displayed average diameter of 233 ± 175 nm and 331 ± 176 nm, respectively ($p < 0.05$).

There was an almost four-fold reduction of fiber diameter with the addition of BR. The elements present in the BR and CeO_2 might have caused the reduction in the fiber diameter of the pristine PU. SEM figures revealed the interaction of beetroot constituents with the polyurethane matrix by a reduction in the size of fiber diameter which is apparently visible. Further, the addition of cerium oxide resulted in a significant decrease in the fiber diameter. The reinforcements added to the polymer matrix appear to be intercalated between the fibers as indicated by arrow marks in the figure. Lakshman et al. fabricated a scaffold based on polyurethane blended with silver nanoparticles. It was reported that the incorporation of silver into the PU resulted in the reduction of the fiber diameter. The reason behind the reduction in the PU fiber diameter was because of an increase in the conductivity of the solution on incorporating silver nanoparticles.[44] Hence, the addition of cerium oxide might have increased the conductivity favoring the reduction of fiber diameter in PU/BR/CeO_2.In a recent study, Prabhakaran fabricated a scaffold based on poly(lactic-co-glycolic acid) (PLGA) added with gelatin for cardiac tissue engineering. It is observed that the addition of gelatin reduces the fiber diameter of PLGA. The obtained fiber diameter is in the range of 630 ± 51 nm to 164 ± 55 nm. This observed range is found suitable for cardiac tissue engineering.[45] The fibre diameter of the fabricated composite is within the above range, suggesting them as a potential candidate for cardiac tissue engineering. Ishii et al. electrospun a nanofibrous mesh based on polycaprolactone (PCL) for cardiac tissue engineering. They reported that the smaller diameter and high surface of the fabricated nanofibrous mesh might be favorable for attachment and proliferation of cardiomyocytes cell.[46] Hence, the fabricated PU/BR and PU/BR/$CeO_2$with smaller fiber diameters compared to the pristine PU might be suitable for the adhesion and proliferation of the cardiomyocytes. Further, the nanofibrous mesh having cerium in the polyurethane matrix and it was determined through an EDX study. Further,

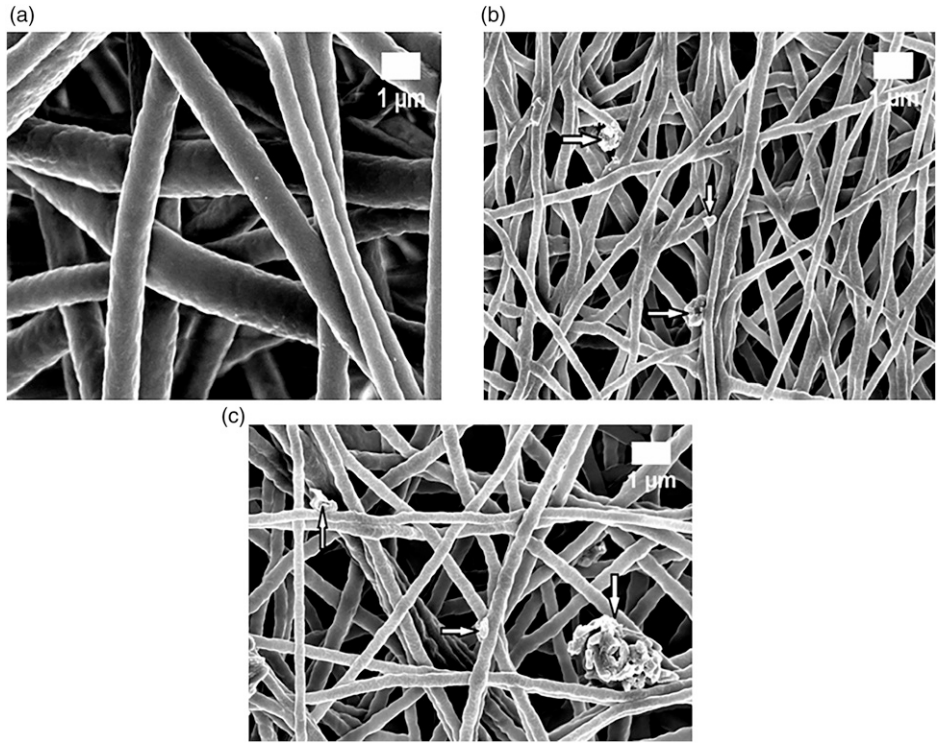

Figure 2. FESEM images of (a) PU, (b) PU/BR, and (c) PU/BR/CeO_2 (arrow mark indicates the intercalation of reinforcements within the polyurethane).

Table 1 indicates the EDX table of electrospun membranes. PU and PU/BR having only carbon and oxygen content while PU/BR/CeO_2 mesh showed some weight percentage of cerium (1.2%) in addition to the carbon and oxygen content.

FTIR analysis

FT-IR spectra of PU, PU/BR, and PU/BR/CeO_2 displayed in Figure 3 and Table 2 denotes the characteristics peak names.[42,43]

PU/BR and PU/BR/CeO_2 displayed similar peaks like that of PU with no new peak formation. However, the addition of BR and CeO_2 decreased the intensity of PU owing to strong hydrogen bond formation.[21] Further, the change in peak shift is observed while adding BR and CeO_2 in the polyurethane matrix.[47] The CH peak at 2920 cm^{-1} was shifted to 2938 cm^{-1} in PU/BR and 2940 cm^{-1} in PU/BR/CeO_2, respectively. The formation of hydrogen bonding and change in peak shift portrays the existence of BR and CeO_2 in the matrix of PU.

Table 1. EDX table of electrospun membranes.

Sample	Carbon (Wt%)	Oxygen (Wt%)	Cerium (Wt%)
PU	77.6	22.2	—
PU/BR	76.8	23.2	—
PU/BR/CeO_2	76.5	22.2	1.2%

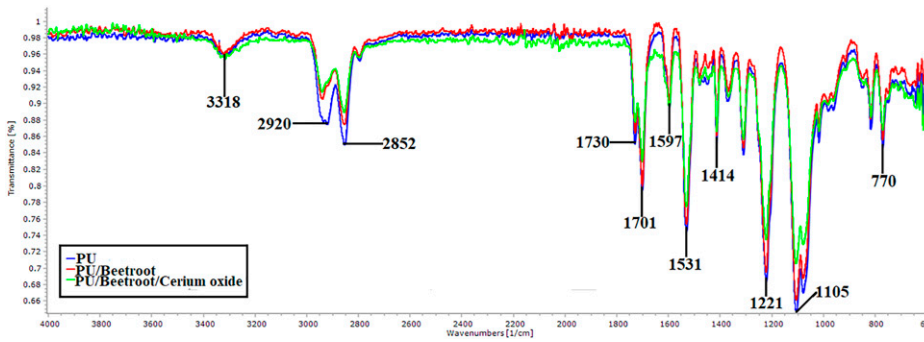

Figure 3. FTIR images of PU, PU/BR, and PU/BR/CeO_2.

Table 2. Characteristic peaks of PU.

S.no	Characteristic peaks	Band name
1	3318 cm^{-1}	NH
2	2920 cm^{-1} and 2852 cm^{-1}	CH
3	1701 cm^{-1} and 1730 cm^{-1}	CO
4	1597 cm^{-1} and 1531 cm^{-1}	NH Vibration
5	1414 cm^{-1}	CH Vibration
6	1221 cm^{-1}, 1105 cm^{-1} and 770 cm^{-1}	CO stretch corresponds to alcohol

Contact angle measurements

The contact angle measurements revealed the angle for the pristine PU was 105° ± 3, while the angle for the PU/BR and PU/BR/CeO_2 was found to be 86° ± 2 and 99° ± 3, respectively ($p < 0.05$). The wettability measurements observed the hydrophobic nature of the polyurethane and it was decreased on adding BR indicating hydrophilic and the angle was increased on adding CeO_2indicating hydrophobic. The most interesting observation is the addition of BR imparted PU as hydrophilic and making hydrophobic on adding CeO_2. Norahan et al. fabricated electroactive graphene oxide (GO) containing collagen (Col) for cardiac tissue engineering. The contact angle of Col, Col–GO-90, and Col–rGO-90 were reported to be 113.3 ± 2.16, 70.06 ± 3.51, and 94.46 ± 2.78, respectively. It was

found that the cell viability of both Col–GO-90 and Col–rGO-90 were reported to be higher.[48] The contact angle of our fabricated composites is found to be overlapping within the reported range and suggesting its feasibility for cardiac tissue growth. Jaganathan et al. developed a cardiac patch using an electrospinning technique based on a polyurethane scaffold added with nickel oxide. They had observed an increase in the hydrophobicity of the PU with the addition of nickel oxide and suggested it as a potential candidate for cardiac tissue engineering.[43] In another recent study, Wang et al. reported the fabrication of PU/poly(ethylene glycol) methacrylate (PEGMA)for vascular applications. The fabricated composites showed hydrophilicity behavior, suggesting potential candidates for vascular applications.[49] Hence, the tailor-made wettability of the fabricated patch materials might be used for cardiac tissue engineering.

Thermal behavior

The thermal behavior of PU, PU/BR, and PU/BR/$CeO_2$is presented in Figure 4. It is observed that PU displayed an initial onset degradation temperature at 284°C and for the electrospun PU/BR and PU/BR/CeO_2, it was estimated to be 289°C and 281°C, respectively. The thermal performance of PU was increased on incorporating BR and on adding CeO_2 it is found to have been decreased owing to the degradation of oxide group present in it. Further, the weight loss peaks of the electrospun PU, PU/BR, and PU/BR/CeO_2were presented in Figure 5. The degradation in PU occurs in three stages, namely, the first loss observed at 220–360°C, the second loss between 360 and 472°C, and the third loss occurs at 472–732°C, respectively. These three losses were because of the decomposition of rigid and flexible segments of the PU. In the electrospun PU/BR composite, it showed four weight losses in which the first loss is observed at 227–331°C, the second loss around 331–367°C, the third loss at 367–492°C, and the fourth loss at 492–817°C.It was noted that in PU/BR composite, the number of weight loss peaks and their peak intensity is increased compared to PU membrane indicating enhanced weight loss. BR containing water molecules which might have resulted in the enhancement of the weight loss. In the case of electrospun PU/BR/CeO_2composite, the weight loss occurs in four stages, namely, first weight loss occurs at 236–374°C, second loss at 374–428°C, third weight loss at 428–489°C, and final loss at 489–654°C, respectively. With the addition of cerium oxide, the numbers of weight loss peaks were the same as that of PU/BR. However, the peak intensity is increased compared to the pristine PU indicating increased weight loss. The change in weight loss peak intensity confirms the presence of BR and CeO_2 in the polyurethane matrix.

Tensile testing

Figure 6 denotes the stress–strain curves of the fabricated patches PU, PU/BR, and PU/BR/CeO_2. PU displayed a tensile strength of 6.16 MPa, while in the case of PU added with BR and BR/CeO_2, the strength was found to be 7.57 MPa and 10.92 MPa, respectively ($p < 0.05$). Further, their mean and standard deviations were given in Table 3.

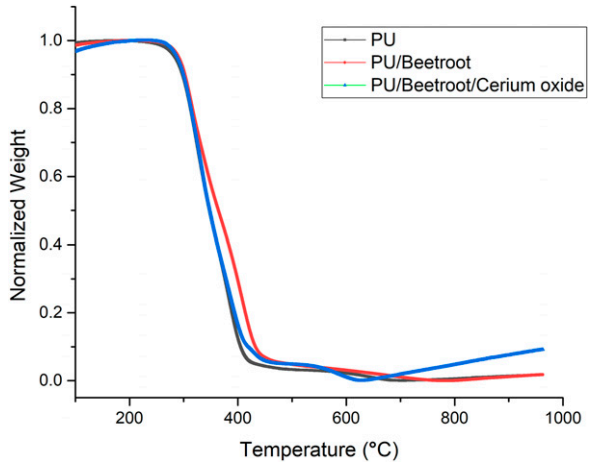

Figure 4. TGA curve of (a) PU, PU/BR, and PU/BR/CeO_2.

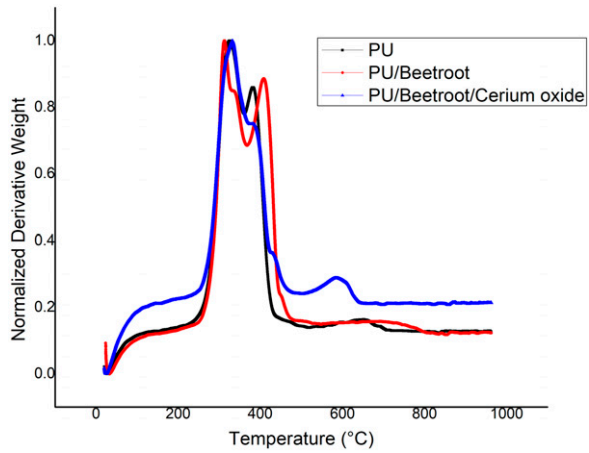

Figure 5. DTG curve of PU, PU/BR, and PU/BR/CeO_2.

It is observed that the tensile strength of the PU is improved by adding BR and CeO_2. The added components might have intercalated with the polyurethane. This might have resulted in bonding between the fibers making them stronger in resisting the fibers break. Chen et al. fabricated polyurethane scaffold added with cellulose for cardiac tissue engineering. It was observed that the addition of cellulose increased the tensile strength of the pristine PU which resembles our findings. The reported tensile strength of PU, P9C1_M, and P9C1_L were reported to be 4.6 ± 1.08, 12.8 ± 3.27, and 8.1 ± 0.67, respectively.[50] Our reported tensile strength was closely matching the reported range

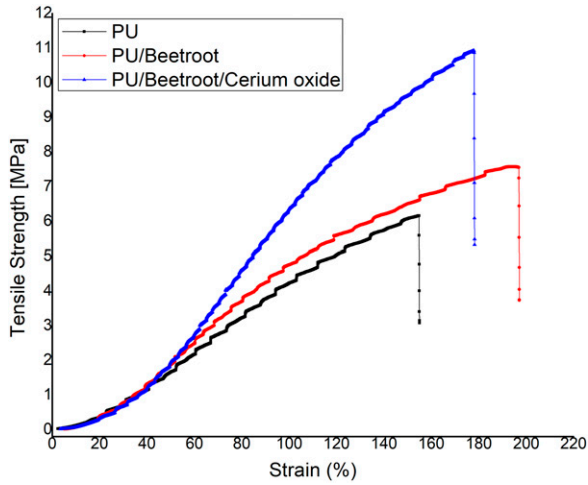

Figure 6. Tensile curves of PU, PU/BR, and PU/BR/CeO_2.

Table 3. Mean and standard deviation of tensile strength for electrospun membranes.

Sample	Tensile strength (MPa)
PU	5.89 ± 0.28
PU/BT	7.71 ± 0.49
PU/BT/CeO_2	10.66 ± 1.03

indicating its suitability for cardiac tissue engineering. Seikh et al. fabricated an electrospun scaffold based on PU/silver nanoparticles and it is found that the addition of additives improved the mechanical strength of PU which resonates with our findings and conclude this might because of their smaller fiber diameter.[51] In this study, the addition of BR and cerium oxide in the pristine PU showed reduced fiber diameter which might have resulted in the enhanced tensile strength.

AFM analysis

AFM images of electrospun PU, PU/BR, and PU/BR/CeO_2wereshown in Figure 7. The measured Ra for the electrospun PU, PU/BR, and PU/BR/CeO_2 was found to be 854 ± 32, 312 ± 12, and 390 ± 125 nm, respectively ($p < 0.05$). Hence, PU surfaces were found to be rougher and become smoother on adding BR and CeO_2. The decrease in the surface roughness can be owed to the interaction of molecules present in BR and CeO_2 with the molecules of pristine PU.As reported in the FTIR study, the interaction of the molecules might cause hydrogen bonding resulting in a decrease in surface roughness. Saporito et al. reported that the scaffold based on gelatin and chondroitin sulfate displayed enhanced adhesion and proliferation of fibroblast cells suggesting it as a potential candidate for

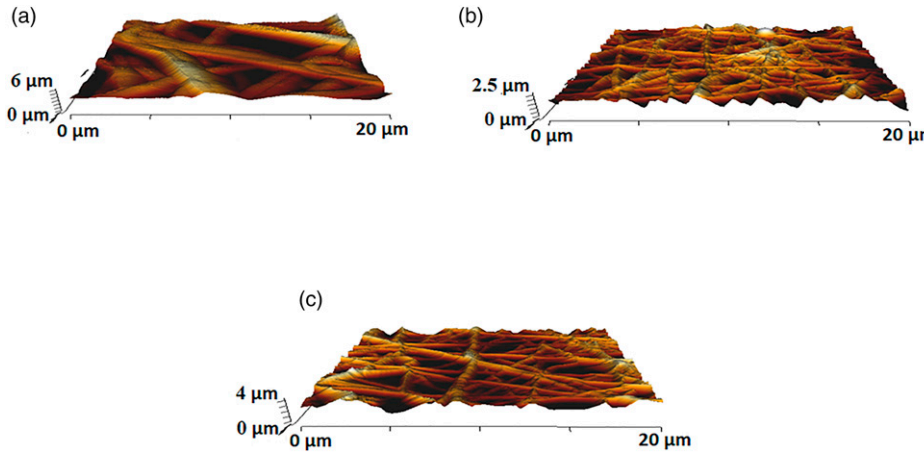

Figure 7. AFM images of (a) PU, (b) PU/BR, and (c) PU/BR/CeO_2.

cardiac tissue growth. In another study, Jang et al. also reported that the electrospun scaffold comprising poly(L-lactide-co-ε-caprolactone) (PLCL) exhibited improved fibroblast cell attachment and proliferation. Hence, the fibroblast cells play a key role in repairing the damaged cardiac tissue.[52,53] Kim et al. investigated the effect of the fiber diameter on the surface roughness of electrospun poly(ε–caprolactone) scaffolds. It had been found that a scaffold with a smaller fiber diameter showed a smoother morphology and became rougher when the diameter became larger.[54] Hence, our fabricated composites showed smaller fiber morphology which might favor the smoother surfaces. It has been reported that the smooth surfaces might favor the enhanced adhesion and proliferation of fibroblast cells.[55] Hence, the smoother surfaces of the developed composites might be used for the new cardiac tissue growth.

Blood compatibility assessments

The anticoagulant behavior of the electrospun membranes is determined through APTT, PT, and hemolytic index and the corresponding images were denoted in Figures 8–10. APTT assay displayed the clotting time for PU is about 176 ± 2 s and for PU added with BR and BR/CeO_2 it is estimated to be 204 ± 3 s, and 205 ± 3 s ($p < 0.05$). Similarly, PT assay displayed the clotting time for PU is about 94 ± 2 s and for PU added with BR and BR/CeO_2, it is found to be 103 ± 2 s, and 105 ± 2 s ($p < 0.05$). Hence, the coagulation assay has depicted the increase in the blood clotting time of the PU on adding BR and CeO_2.

Further, the hemolytic assay was done to evaluate the hemoglobin release from the electrospun patches. The hemolytic assay measurements depicted the PU membranes added with BR and PU/BR/CeO_2 patches showed less toxic behavior to the RBC's. The hemolytic index of the pristine PU was found to be 2.83%, while the PU having BR and BR/CeO_2 nanofibers showed hemolytic index of 1.633% and 1.74%, respectively

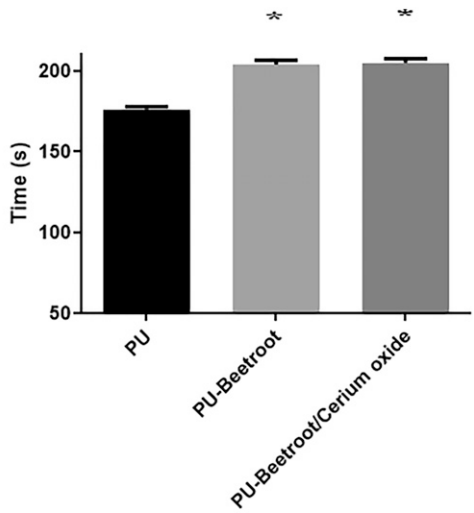

Figure 8. APTT measurements of PU, PU/BR, and PU/BR/CeO_2.

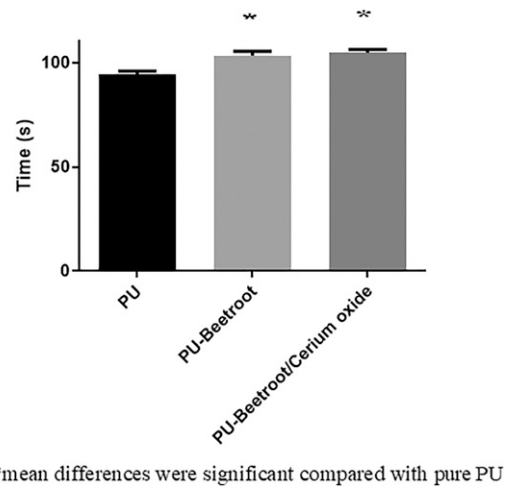

Figure 9. PT measurements of PU, PU/BR, and PU/BR/CeO_2.

($p < 0.05$). Hence, the composite materials were considered as non-hemolytic nature (index below 2%) according to ASTMF756-00(2000).[42,43] Jaganathan et al. prepared an electrospun scaffold based on polyurethane added with *Alternanthera sessilis* oil (AS). The addition of AS oil improved the blood clotting time of the PU which resembles our

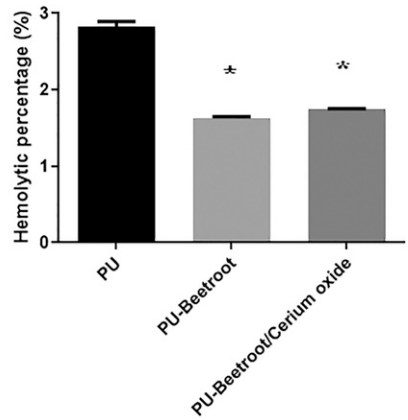

Figure 10. Hemolytic index of PU, PU/BR, and PU/BR/CeO_2.

findings. They concluded this behavior was owing to their smaller fiber diameter and hydrophobic behavior.[42] In our study, the electrospun nanocomposites displayed smaller fiber diameter (PU/BR and PU/BR/CeO_2) and hydrophobic (PU/BR/CeO_2) behavior which might have favored the enhanced blood compatibility.

Conclusion

The cardiac patch requires materials with tailor-made properties to suit its function. This work developed PU/BR and PU/BR/CeO_2 patches with adequate properties mimicking the extracellular matrix of the cardiac tissue via:

- Nanofibrous morphology (Decrement percentage was 77% for PU/BT and 67% for PU/BT/CeO2 compared to the pristine PU) and altered wettability of the fabricated composites compared to the pristine PU.
- Reduced surface roughness (Decrement percentage was 63% for PU/BR and 54% for PU/BR/CeO2) and enhanced tensile strength (Percentage increment was 23% for PU/BR and 77% for PU/BR/CeO2 compared to the pristine PU) of the electrospun composites compared to the pristine PU.
- Blood coagulation and hemolysis assay showed its antithrombogenic (Percentage increment was 16% for both PU/BT and PU/BT/CeO2in APTT assay and in PT assay, the percentage increment was 10% for PU/BT and 12% for PU/BT/CeO2) and less toxic nature of the fabricated composites than the pristine PU.
- Hence, the electrospun PU/BR and PU/BR/CeO2 nanocomposite with tailor-made characteristics indicating its potential benefits for cardiac patch applications.

Declaration of conflicting interests

The author(s) declared no potential conflicts of interest with respect to the research, authorship, and/or publication of this article.

Funding

The author(s) disclosed receipt of the following financial support for the research, authorship, and/or publication of this article: Ahmad Athif Mohd Fauzi would like to acknowledge the grant (vot.no QJ130000.21A6.00P13) funded by Ministry of Higher Education, Malaysia.

ORCID iD

Saravana K Jaganathan https://orcid.org/0000-0002-2785-137X

References

1. Ahmed N. *Pathophysiology of Ischemia Reperfusion Injury and Use of Fingolimod in Cardioprotection*. USA: Acad Press, 2019.
2. Ong SB, Hernández-Reséndiz S, Crespo-Avilan GE, et al. Inflammation following acute myocardial infarction: multiple players, dynamic roles, and novel therapeutic opportunities. *Pharmacol Ther* 2018; 186: 73–87.
3. French BA and Kramer CM. Mechanisms of postinfarct left ventricular remodeling. *Drug Discov Today Dis Mech* 2007; 4(3): 185–196.
4. Varma P, Krishna N, Jose R, et al. Ischemic mitral regurgitation. *Ann Card Anaesth* 2017; 20(4): 432.
5. Masarone D, Limongelli G, Rubino M, et al. Management of arrhythmias in heart failure. *J Cardiovasc Dev Dis* 2017; 4(1): 3.
6. Chew HC. *Enhanced recovery of donor hearts*. Australia: Doctoral dissertation, Victor Chang Cardiac Research Institute.
7. Secretariat MA. Primary angioplasty for the treatment of acute st-segment elevated myocardial infarction: an evidence-based analysis. *Ont Health Technol Assess Ser* 2004; 4(10): 1–65.
8. Hashimoto H, OlsonEN andBassel-Duby EN and Bassel-Duby R. Therapeutic approaches for cardiac regeneration and repair. *Nat Rev Cardiol* 2018; 15(10): 585–600.
9. Yalcin I, Horakova J, Mikes P, et al. Design of polycaprolactone vascular grafts. *J Ind Text* 2016; 45(5): 813–833.
10. Zhang J. Engineered tissue patch for cardiac cell therapy. *Curr Treat Options Cardiovasc Med* 2015; 17(8): 37.
11. Li H, Bao M and Nie Y. Extracellular matrix-based biomaterials for cardiac regeneration and repair. *Heart Fail Rev* 2021; 26(5): 1231–1248.
12. Shi X, Zhou W, Ma D, et al. Electrospinning of nanofibers and their applications for energy devices. *J Nanomater* 2015; 2015: 140716.
13. Alghoraibi I and Alomari S. Different methods for nanofiber design and fabrication. *Handbook of Nanofibers*. Cham, Switzerland: Springer, 2018, pp. 1–46.
14. Mirek A, Korycka P, Grzeczkowicz M, et al. Polymer fibers electrospun using pulsed voltage. *Mater Des* 2019; 183: 108106.

15. Vasita R and Katti DS. Nanofibers and their applications in tissue engineering. *Int J Nanomedicine* 2006; 1(1): 15–30.
16. Liu H, Ding X, Zhou G, et al. Electrospinning of nanofibers for tissue engineering applications. *J Nanomater* 2013; 2013.
17. Balan KK and Sundaramoorthy S. Hydroentangled nonwoven eri silk fibroin scaffold for tissue engineering applications. *J Ind Text* 2019; 48(8): 1291–1309.
18. Dhandayuthapani B, Yoshida Y, Maekawa T, et al. Polymeric scaffolds in tissue engineering application: a review. *Int J Polym Sci* 2011; 2011.
19. Joseph J, Patel RM, Wenham A, et al. Biomedical applications of polyurethane materials and coatings. *Trans IMF* 2018; 96(3): 121–129.
20. Gabriel LP, Rodrigues AA, Macedo M, et al. Electrospun polyurethane membranes for tissue engineering applications. *Mater Sci Eng C* C2017; 72: 113–117.
21. Unnithan AR, Pichiah PBT, Gnanasekaran G, et al. Emu oil-based electrospun nanofibrous scaffolds for wound skin tissue engineering. *Colloids Surf A Physicochem Eng Asp* 2012; 415: 454–460.
22. Augustine R, Dan P, Sosnik A, et al. Electrospun poly(vinylidene fluoride-trifluoroethylene)/zinc oxide nanocomposite tissue engineering scaffolds with enhanced cell adhesion and blood vessel formation. *Nano Res* 2017; 10(10): 3358–3376.
23. Amer S, Attia N, Nouh S, et al. Fabrication of sliver nanoparticles/polyvinyl alcohol/gelatin ternary nanofiber mats for wound healing application. *J Biomater Appl* 2020; 35(2): 287–298.
24. Nelson B, Johnson M, Walker M, et al. Antioxidant cerium oxide nanoparticles in biology and medicine. *Antioxidants* 2016; 5(2): 15.
25. Dhall A and Self W. Cerium oxide nanoparticles: a brief review of their synthesis methods and biomedical applications. *Antioxidants* 2018; 7(8): 97.
26. Kargozar S, Baino F, Hoseini SJ, et al. Biomedical applications of nanoceria: new roles for an old player. *Nanomedicine* 2018; 13(23): 3051–3069.
27. Nyoka M, Choonara YE, Kumar P, et al. Synthesis of cerium oxide nanoparticles using various methods: implications for biomedical applications. *Nanomaterials* 2020; 10(2): 242.
28. Liu RH. Potential synergy of phytochemicals in cancer prevention: mechanism of action. *J Nutr* 2004; 134(12): 3479S–3485S.
29. El Gamal AA, AlSaid MS, Raish M, et al. Beetroot (Beta vulgaris L.) extract ameliorates gentamicin-induced nephrotoxicity associated oxidative stress, inflammation, and apoptosis in rodent model. *Mediators Inflamm* 2014; 2014: 983952.
30. *Nutrient Data for Beets, Raw Per 100 G*. United States Department of Agriculture, National Nutrient Database, release SR-28. 2016. Retrieved 20 March 2017.
31. Available at: https://en.wikipedia.org/wiki/Beetroot
32. Mirmiran P, Houshialsadat Z, Gaeini Z, et al. Functional properties of beetroot (Beta vulgaris) in management of cardio-metabolic diseases. *Nutr Metab* 2020; 17(1): 3–5.
33. Hekmat M, Kenawy SH and Khalil AM. Betanin: a promising molecule for biomedical applications. *Bioint Res Appl Chem* 2020; 10(3): 5392–5399. DOI: 10.33263/BRIAC103.392399.
34. Nahla TK, Wisam SU and Tariq NM. Antioxidant activities of beetroot (Beta vulgaris L.) extracts. *Pakistan J Nutr* 2018; 17: 500–505.

35. Rajeshkumar S and Naik P. Synthesis and biomedical applications of Cerium oxide nanoparticles - a review. *Biotechnol Rep* Rep2018; 17: 1–5.
36. Urner M, Schlicker A, Z'graggen BR, et al. Inflammatory response of lung macrophages and epithelial cells after exposure to redox active nanoparticles: effect of solubility and antioxidant treatment. *Environ Sci Technol* 2014; 48(23): 13960–13968.
37. Fisichella M, Berenguer F, Steinmetz G, et al. Toxicity evaluation of manufactured CeO2 nanoparticles before and after alteration: combined physicochemical and whole-genome expression analysis in Caco-2 cells. *BMC Genomics* 2014; 15(1): 700.
38. Franchi LP, Manshian BB, de Souza TAJ, et al. Cyto- and genotoxic effects of metallic nanoparticles in untransformed human fibroblast. *Toxicol Vitro* 2015; 29(7): 1319–1331.
39. Dhall A and Self W. Cerium oxide nanoparticles: a brief review of their synthesis methods and biomedical applications. *Antioxidants* 2018; 7(8): 97.
40. Alpaslan E, Yazici H, Golshan NH, et al. pH-dependent activity of dextran-coated cerium oxide nanoparticles on prohibiting osteosarcoma cell proliferation. *ACS Biomater Sci Eng* 2015; 1(11): 1096–1103.
41. Nyoka M, Choonara YE, Kumar P, et al. Synthesis of cerium oxide nanoparticles using various methods: implications for biomedical applications. *Nanomaterials* 2020; 10(2): 242.
42. Jaganathan SK and Mani MP. Development and blood compatibility evaluation of novel fibrous textile scaffold based on polyurethane amalgamated with Alternanthera sessilis oil for the bone tissue engineering. *J Indus Text* 2020: 1528083720906809.
43. Jaganathan SK and Mani MP. Enriched mechanical, thermal, and blood compatibility of single stage electrospun polyurethane nickel oxide nanocomposite for cardiac tissue engineering. *Polym Composites* 2019; 40(6): 2381–2390.
44. Lakshman LR, Shalumon KT, Nair SV, et al. Preparation of silver nanoparticles incorporated electrospun polyurethane nano-fibrous mat for wound dressing. *J Macromol Sci A* 2010; 47(10): 1012–1018.
45. P Prabhakaran M, Kai D, Ghasemi-Mobarakeh L, et al. Electrospun biocomposite nanofibrous patch for cardiac tissue engineering. *Biomed Mater* 2011; 6(5): 055001.
46. Ishii O, Shin M, Sueda T, et al. In vitro tissue engineering of a cardiac graft using a degradable scaffold with an extracellular matrix-like topography. *J Thorac Cardiovasc Surg* 2005; 130: 1358–1363.In
47. Tijing LD, Ruelo MTG, Amarjargal A, et al. Antibacterial and superhydrophilic electrospun polyurethane nanocomposite fibers containing tourmaline nanoparticles. *Chem Eng J* 2012; 197: 41–48.
48. Norahan MH, Amroon M, Ghahremanzadeh R, et al. Electroactive graphene oxide-incorporated collagen assisting vascularization for cardiac tissue engineering. *J Biomed Mater Res A* 2019; 107(1): 204–219.
49. Wang H, Feng Y, An B, et al. Fabrication of PU/PEGMA crosslinked hybrid scaffolds by in situ UV photopolymerization favoring human endothelial cells growth for vascular tissue engineering. *J Mater Sci Mater Med* 2012; 23(6): 1499–1510.
50. Chen P-H, Liao H-C, Hsu S-H, et al. A novel polyurethane/cellulose fibrous scaffold for cardiac tissue engineering. *RSC Adv* 2015; 5(9): 6932–6939.

51. Sheikh FA, Barakat NAM, Kanjwal MA, et al. Self synthesize of silver nanoparticles in/on polyurethane nanofibers: Nano-biotechnological approach. *J Appl Polym Sci* 2010; 115(6): 3189–3198.
52. Saporito F, Sandri G, Bonferoni MC, et al. Electrospun gelatin-chondroitin sulfate scaffolds loaded with platelet lysate promote immature cardiomyocyte proliferation. *Polymers* 2018; 10(2): 208.
53. Jang BS, Cheon JY, Kim SH, et al. Small diameter vascular graft with fibroblast cells and electrospun poly (L-lactide-co-ε-caprolactone) scaffolds: cell matrix engineering. *J Biomater Sci Polym Ed* 2018; 29(7–9): 942–959.
54. Kim HH, Kim MJ, Ryu SJ, et al. Effect of fiber diameter on surface morphology, mechanical property, and cell behavior of electrospun poly(ε-caprolactone) mat. *Fibers Polym* 2016; 17(7): 1033–1042.
55. Huag H-S, Chou S-H, Don T-M, et al. Formation of microporous poly(hydroxybutyric acid) membranes for culture of osteoblast and fibroblast. *Polym Adv Tech* 2009; 20(12): 1082–1090.